Journal of Hepatocellular Carcinoma

Dovepress
Taylor & Francis Group

Open Access Full Text Article

ORIGINAL RESEARCH

A Preoperative MRI-Based Score to Predict High-Risk Pathology and Stratify Adjuvant Therapy Benefit in BCLC 0/A Hepatocellular Carcinoma

Huiying Li[1], Xinxin Wang[1], Can Yu[1], Baihe Li[1], Zhe Hu[1], Wanhu Li[2], Yueqin Chen[3], Yang Zhou[1], Yajuan Sun[1]

[1]Department of Radiology, Harbin Medical University Cancer Hospital, Harbin, Heilongjiang, 150081, People's Republic of China; [2]Department of Radiology, Shandong Provincial Cancer Hospital, Jinan, Shandong, 250000, People's Republic of China; [3]Department of Radiology, Affiliated Hospital of Jining Medical University, Jining, Shandong, 272007, People's Republic of China

Correspondence: Yajuan Sun; Yang Zhou, Email yajuan-sun@163.com; zhouyang094@126.com

Purpose: This study aims to develop and validate a magnetic resonance imaging (MRI)-based preoperative scoring model for predicting microvascular invasion (MVI) or Edmondson–Steiner grade 3/4 in BCLC 0/A hepatocellular carcinoma (HCC) and explore its potential for early recurrence risk stratification and as a hypothesis-generating tool for identifying patients who may benefit from adjuvant therapy.

Materials and Methods: This multicenter retrospective study comprised consecutive patients with BCLC 0/A HCC who underwent contrast-enhanced MRI followed by curative resection at three different institutions between January 2015 and November 2024. To identify imaging predictors of MVI and Edmondson–Steiner grade 3/4, multivariable logistic regression was applied to the training set. Imaging features and AFP levels were combined to create a scoring system (HRI-score), and the model's ability to predict recurrence and stratify recurrence-free survival (RFS) was assessed in internal and external sets.

Results: Overall, 994 patients were included (training: n = 601; internal validation: n = 257; external outcome set: n = 136). The HRI-score included irregular tumor morphology, nonperipheral washout, intratumoral blood products, and AFP (≥ 400 ng/mL). The training and internal validation sets had AUCs of 0.813 and 0.747, respectively. Across all sets, RFS was significantly lower in HRI-positive patients than for HRI-negative patients (all $P < 0.05$). Adjuvant therapy was associated with improved RFS in the HRI-positive subgroup; however, this effect was not observed in the HRI-negative subgroup, based on exploratory analyses.

Conclusion: The HRI-score enables preoperative prediction of high-risk pathological features and risk stratification in BCLC 0/A HCC. It may also serve as a hypothesis-generating tool to identify patients who could potentially benefit from adjuvant therapy, warranting further prospective multicenter validation.

Keywords: hepatocellular carcinoma, magnetic resonance imaging, microvascular invasion, Edmondson-Steiner, Chinese medicine

Introduction

Liver resection is currently the main treatment for BCLC 0/A hepatocellular carcinoma (HCC) in patients with well-preserved liver function.[1] However, the 5-year recurrence rate is still high at 59.3% even following curative liver resection.[2] Microvascular invasion (MVI) and Edmondson-Steiner G3/4 have been confirmed as significant risk factors for postoperative recurrence and poor prognosis.[3–5]

To address the clinical challenge of high postoperative recurrence risk in patients with BCLC stage 0/A HCC, domestic and international guidelines recommend that adjuvant therapy should be considered for HCC patients with high-risk recurrence factors.[6–8] Studies indicate that various adjuvant treatments may be effective in lowering recurrence rates following liver resection; however, to date, no standardized regimen that is both widely accepted and clearly effective has been established. Traditional Chinese medicine preparations (such as Huaier granules) have been referenced in some Chinese HCC management guidelines' recommendations for postoperative adjuvant therapy.[7] According to

https://doi.org/10.2147/JHC.S605420
Received: 2 March 2026
Accepted: 13 May 2026
Published: 22 May 2026

previous studies, Huaier granules may improve disease-free survival and reduce recurrence rates.[9–11] However, clear criteria for identifying the patient population that may benefit from this treatment are still lacking.

Tumor multiplicity, large tumor size (such as > 5 cm), macrovascular invasion, MVI, and Edmondson-Steine G3/4 are commonly identified as high-risk recurrence factors.[12,13] MVI and Edmondson-Steiner grade still depend on postoperative pathological analysis, even though tumor number, size, and macrovascular invasion can be relatively easily determined through preoperative imaging. As a result, developing optimal surgical plans preoperatively becomes challenging. Additionally, there is significant variability in this "high-grade pathological" group. Some patients experience a rapid recurrence despite adjuvant therapy, while others may have their treatment needs underestimated. This implies that identifying which patients would actually benefit from adjuvant therapy may be insufficient if postoperative pathological analysis is the only method used.

According to recent research, various magnetic resonance imaging (MRI) characteristics are closely linked to high-risk pathological (HRP) features of HCC and can be used as noninvasive tools to predict HCC prognosis. For instance, irregular tumor morphology is thought to be a significant predictor of MVI,[14] and nonperipheral washout indicates Edmondson-Steiner G3/4.[15,16] The clinical utility of MRI features in predicting multiple HRP characteristics and identifying potential beneficiaries of postoperative adjuvant therapy among BCLC 0/A patients undergoing curative resection remains incompletely validated, and the existing research mainly focuses on evaluating single pathological outcomes;[17–19] most studies have focused on patients with locally advanced HCC.

Therefore, the main goal of this research is to create and validate a useful scoring system based on serum biomarkers and MRI features for the noninvasive preoperative prediction of HRP characteristics in HCC. Additionally, the clinical utility of this scoring system includes predicting recurrence-free survival (RFS) after curative resection and identifying patients who may benefit from adjuvant therapy. This aspect represents another key goal of the study.

Materials and Methods

Patients

This multicenter retrospective study included patients diagnosed with HCC who underwent hepatectomy at three medical centers in China: Harbin Medical University Cancer Hospital, the Affiliated Hospital of Jining Medical University, and Shandong Provincial Cancer Hospital.

Patients with HCC who underwent hepatectomy at Harbin Medical University Cancer Hospital between January 2015 and November 2024 were considered for inclusion. The inclusion criteria were as follows: (a) Age ≥ 18 years; (b) pathologically confirmed BCLC 0/A HCC; (c) contrast-enhanced MRI performed within 2 weeks before surgery. The exclusion criteria were as follows: (a) Receiving any HCC-related treatment prior to the initial MRI examination; (b) poor image quality; (c) any malignancy other than HCC, either present or in the past; (d) incomplete clinical data, laboratory indices, or pathological information. Following data integration, the study population (n = 858) was randomly divided into a training set (n = 601) and an internal validation set (n = 257) in a 7:3 ratio. Additionally, the same inclusion and exclusion criteria were used on an external outcome set from two other hospitals between January 2020 and November 2024, yielding a total of 136 patients. As a result, this study included 994 patients in total (Figure 1).

Image Acquisition and Analysis

MRI was conducted using 3.0 T MRI scanners. Table S1 presents a thorough explanation of MRI acquisition parameters used in this study. To further minimize potential variability introduced by various scanners and contrast administration protocols, all imaging data were centrally gathered and examined using a standardized post-processing workflow.

Two radiologists (*Y. J. S.* and *Y. Z.*, with 17 and 21 years of experience in liver MRI, respectively) independently analyzed MRI scans. Both readers were blinded to pathological and clinical data. Tumor shape (regularity type or irregularity type) and other previously published prognostic imaging features (Table S2) were among MRI features evaluated using the Liver Imaging Reporting and Data System (LI-RADS) version 2018 criteria.[20] For all image features, agreement between and within the readers was assessed. In the case of disagreement on qualitative parameters, the two

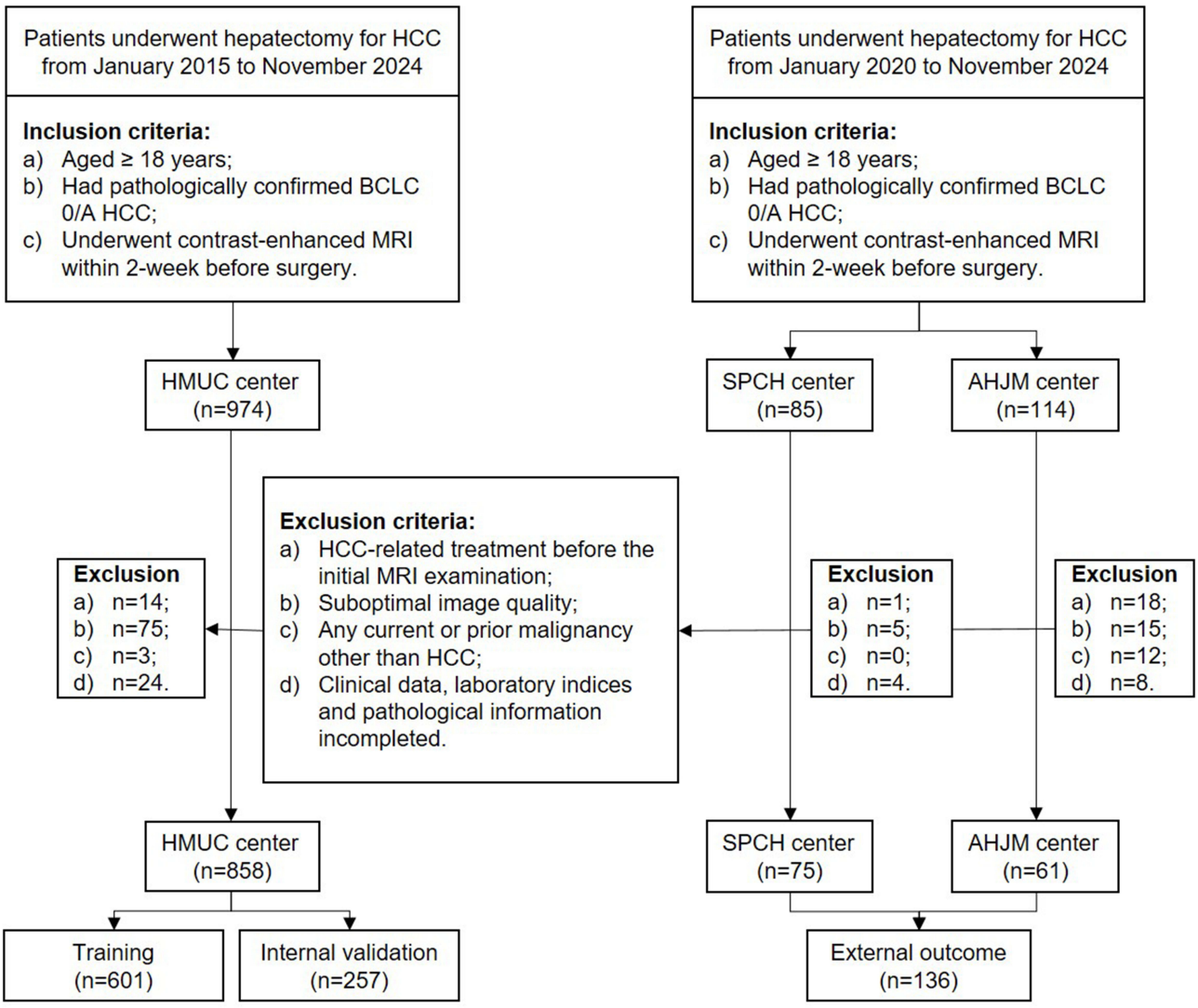

Figure 1 Flow chart of the study population.
Abbreviations: HCC, hepatocellular carcinoma; MRI, magnetic resonance imaging; BCLC, Barcelona Clinic Liver Cancer; HMUC, Harbin Medical University Cancer Hospital; SPCH, Shandong Provincial Cancer Hospital; AHJM, Affiliated Hospital of Jining Medical University.

readers discussed the data and used the consensus finding for further analysis. Data from the senior reader were statistically analyzed for quantitative parameters (Table S3).

Clinical Data and Pathological Examination

Gathered preoperative clinical data, such as gender, age, AFP, cirrhosis, and HCV. Standard clinical laboratory reference ranges were used to dichotomize all relevant biochemical variables, with the upper limit of normal serving as the threshold. MVI status and Edmondson-Steiner grade were determined using histopathologic data from routine reports as the reference standard. At each center, a consensus review of all specimens was conducted by two liver pathologists who were aware of the clinical and imaging data in accordance with the institutional standard procedures. The presence of MVI or Edmondson-Steiner G3/4 was considered an HRP feature.

Follow Up

Following curative surgery, all patients were monitored in accordance with institutional practice, which includes laboratory examinations such as serum AFP every 3 months and CT/MRI every 3 to 6 months. Unequivocal radiological

https://doi.org/10.2147/JHC.S605420

or pathological detection of intrahepatic HCC, tumor-in-vein, or distant metastasis was considered a recurrence.[3] RFS was defined from the date of SR until the last follow-up visit or recurrence. The data were censored on Jun 25, 2025.

Postoperative Adjuvant Treatment

Based on Chinese guidelines for the treatment of primary liver cancer,[7,8] adjuvant treatment decisions were made for patients who had a high risk of postoperative recurrence/metastasis: Tumor diameter of > 5 cm, multifocal tumors, MVI, macrovascular invasion, lymph node metastasis, and Edmondson-Steiner G3/4. Transarterial chemoembolization, hepatic arterial infusion chemotherapy, targeted therapy, immunotherapy, traditional Chinese medicine (TCM), and combined therapy were among the adjuvant treatment options (Table S4).

HRI Development and Validation

A scoring system for predicting HRP in patients with HCC was created using the training set. Three steps comprised the interpretable high-risk image (HRI) tool (Table S5). Initially, AFP and imaging features linked with each HRP were identified, and their weight parameters (β-value) were obtained using multivariable logistic regression analysis. Kendall's tau-b test was then used to assess the correlations between each HRP and recurrence, and the correlation coefficients (r_{MVI}, $r_{E\text{-}S\ G3/4}$) were combined with the β-value. Finally, to predict HRP in HCC, features were given values, and a scoring model was created by combining these values to produce a continuous HRI feature score (HRI-score). The HRI-score threshold was determined using the optimal area under the receiver operating characteristic curve (AUC) for HRP prediction. The HRI-score was deemed positive when it exceeded the threshold value and negative otherwise. The effectiveness of HRI-score in the validation set was also assessed.

Statistical Analysis

AUC, sensitivity, specificity, positive predictive value (PPV), negative predictive value (NPV), and accuracy were used to assess the discrimination of the HRI-score system. The RFS of patients using the HRI-score was calculated using a Kaplan–Meier plot with Log rank tests. Statistical significance was defined as two-sided *P*-values < 0.05. Decision curve analysis (DCA), clinical impact curve, and calibration curves were used to assess the clinical utility of HRI-score system. Time-dependent ROC curves were used to evaluate the prognostic performance of HRI-score at 1-, 2-, and 3-year time points. Censoring was handled using the inverse probability of censoring weighting method implemented in the "timeROC" package. To assess model stability and potential overfitting, bootstrap resampling with 200 iterations was performed to obtain optimism-corrected AUCs. Propensity score-matching (PSM) analysis was utilized to reduce potential confounding and the impact of selection bias by equating the two groups based on the presence of MVI. A nearest-neighbor 1:3 matching scheme with a caliper size of 0.2 was employed for propensity score matching. The data were analyzed and presented using R (version 4.4.2; R Foundation for Statistical Computing).

Results

Baseline Characteristics

The study sets consisted of the training set (n = 601), the internal validation set (n = 257), and the external outcome set (n = 136). With proportions of 80.2% in the training set, 80.54% in the internal validation set, and 94.85% in the external outcome set, most patients had hepatitis B virus infection. Table 1 contains detailed baseline characteristics. MVI and Edmondson-Steiner G3/4 tumors were found in 215 (35.77%) and 470 (78.2%) patients in the training set and in 87 (33.85%) and 193 (75.1%) patients in the internal validation set. Recurrence was observed in 253 patients (42.09%) in the training set, 105 (40.85%) in the internal validation set, and 34 (25.0%) in the external outcome set. Postoperative medication was given to 304 (35.4%) patients.

Development of the HRI-Score

Table S6 summarizes the results of univariate logistic regression. AFP ≥ 400 ng/mL, irregular tumor shape, and nonperipheral washout were all independently associated with MVI in multivariable analysis. Independent predictors for Edmondson-Steiner G3/4 included AFP ≥ 400 ng/mL, irregular tumor shape, intratumoral blood products, and nonperipheral

Table 1 Baseline Patient Characteristics

Variables	Training Set (N=601)	Internal validation Set (N=257)	External Outcome Set (N=136)	*P*-value
Sex				0.24[a]
Female	121 (20.13)	44 (17.12)	33 (24.26)	
Male	480 (79.87)	213 (82.88)	103 (75.74)	
Age (years)	58 (52, 64)	59 (53, 64)	59 (52, 66)	0.90[a]
AFP (ng/mL)				0.05[a]
<400	466 (77.54)	186 (72.37)	113 (83.09)	
≥400	135 (22.46)	71 (27.63)	23 (16.91)	
Underlying liver diseases				<0.01[a]
No	63 (10.48)	33 (12.84)	4 (2.94)	
Hepatitis B virus	482 (80.20)	207 (80.54)	129 (94.85)	
Others	56 (9.32)	17 (6.61)	3 (2.21)	
Cirrhosis				<0.01[a]
Absent	88 (14.64)	48 (18.68)	5 (3.68)	
Present	513 (85.36)	209 (81.32)	131 (96.32)	
Tumor size (mm)	42 (30, 62)	41 (28, 62)	38.5 (23.75, 53.5)	0.05[a]
Tumor multiplicity				0.15[a]
1	579 (96.34)	244 (94.94)	136 (100.00)	
2	19 (3.16)	11 (4.28)	0 (0.00)	
≥3	3 (0.50)	2 (0.78)	0 (0.00)	
MVI				0.644[b]
Negative	386 (64.23)	170 (66.15)	NA	
Positive	215 (35.77)	87 (33.85)	NA	
Edmondson-Steiner grade				0.365[b]
G1/2	131 (21.80)	64 (24.90)	NA	
G3/4	470 (78.20)	193 (75.10)	NA	

Notes: Data in parentheses are percentages or interquartile ranges. [a]*P*-values were calculated by comparing the training set (n = 601), internal validation set (n = 257), and external validation set (n = 136).[b]*P*-values were computed by comparing the training (n = 601) and internal validation (n = 257) sets. NA denotes missing data.
Abbreviations: AFP, α-fetoprotein; MVI, Microvascular invasion.

washout. A weighted scoring system was developed based on these characteristics. To determine feature weights, correlation coefficients for MVI (r = 0.087) and tumor grade (r = 0.148) were multiplied by the corresponding regression coefficients (β-value, Table 2). The continuous HRI-score was then generated by converting these weights to point values (Figure 2).

Table 2 Training Center Multivariable Logistic Regression Analyses Based on Majority Interpretations

	Multivariable Analysis		
	β Coefficient	OR (95% CI)	*P*-value
Microvascular invasion			
AFP (≥400 ng/mL)	0.48	1.62(1.07–2.44)	0.0218
Tumor shape (irregularity)	0.79	2.21(1.53–3.19)	<0.001
Nonperipheral washout (present)	0.97	2.63(1.23–5.65)	0.0131
Edmondson-Steiner G3/4			
AFP (≥400 ng/m)	1.13	3.1(1.6–6.02)	<0.001
Tumor shape (irregularity)	1.38	3.99(2.3–6.89)	<0.001
Blood products in mass (present)	1.05	2.84(1.54–5.24)	<0.001
Nonperipheral washout (present)	1.34	3.82(1.98–7.38)	<0.001

Note: Interpretations.
Abbreviations: OR, Odds ratio; CI, Confidence intervals; AFP, α-fetoprotein.

Sensitivity of the HRI-Score

The HRI-score was deemed positive when it exceeded four and negative otherwise. The HRI-score displayed strong discrimination for HRP using this threshold: In the training set, the AUC was 0.813 (95% CI: 0.778–0.849), and in the internal validation set, the AUC was 0.747 (0.684–0.811). The classification metrics (accuracy, sensitivity, specificity, PPV, and NPV) at this cut-off are summarized in Table 3. The model's clinical utility across a range of decision thresholds was further supported by calibration curves, DCA, and a clinical impact curve (Figure S1). With AUC values of 0.71 for 1-year survival, 0.68 for 2-year survival, and 0.66 for 3-year survival predictions, respectively, the model demonstrated good discrimination in the internal validation set (Figure S1).

Clinical Significance of the HRI-Score

Patients who are HRI-positive had significantly lower RFS than patients who are HRI-negative when patients were stratified by HRI status in the training set ($P < 0.0001$), internal validation set ($P = 0.036$), and external outcome set ($P = 0.047$) (Figure 3A–C). In training and internal validation sets, patients who are HRP-positive had worse RFS than patients who are HRP-negative, which is consistent with its correlation with adverse pathology (Figure 3D and E). Based on their HRP and HRI status, patients were divided into four groups. All four groups displayed a progressive decline in

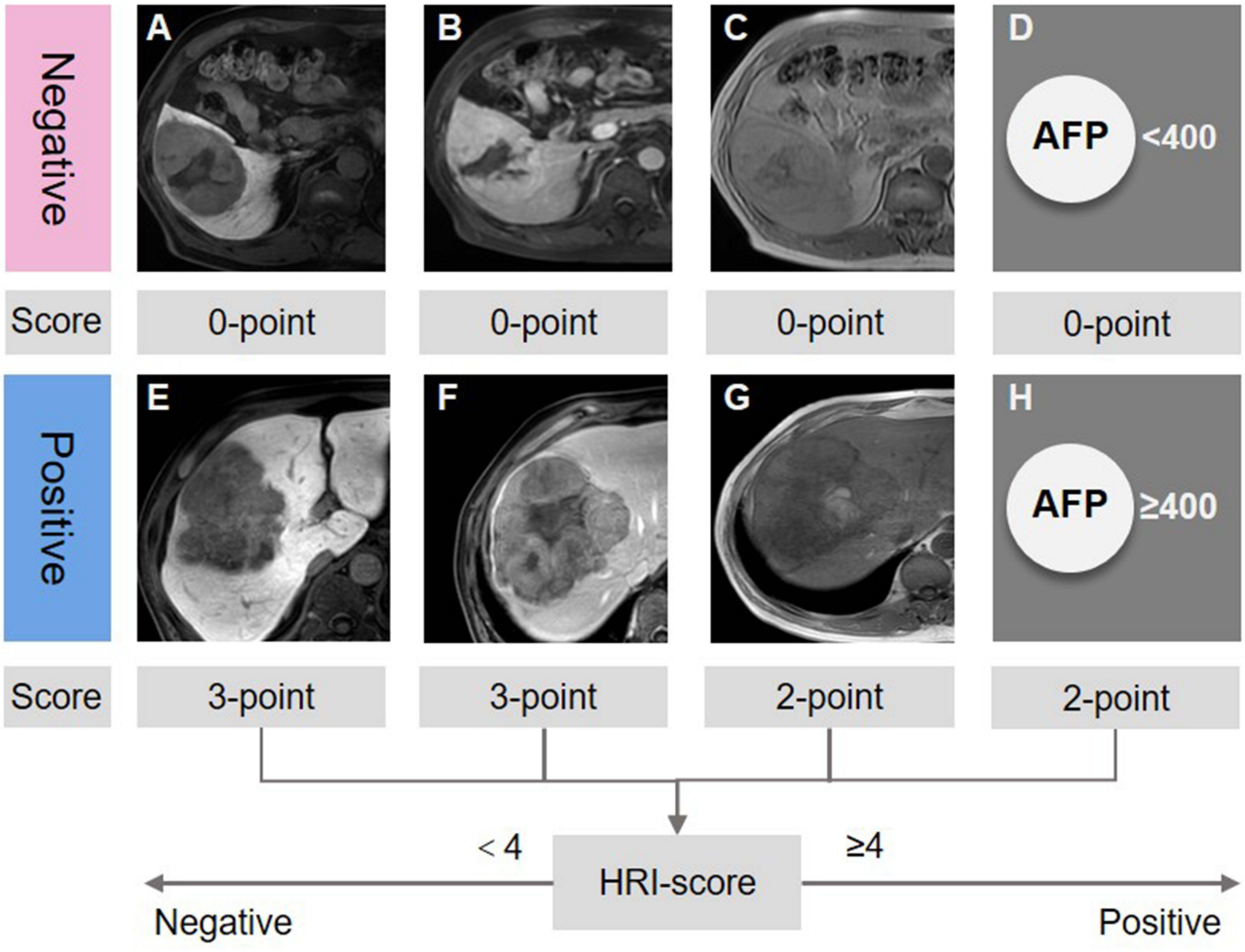

Figure 2 Assignment of the HRI-score based on imaging features assessed on contrast–enhanced MRI scans. (**A–D**) Imaging features representing zero points: (**A**) regular shape, (**B**) no nonperipheral washout, (**C**) no blood products in mass, and (**D**) AFP<400ng/mL. (**E–H**) Imaging features representing added points: (**E**) three points for irregular shape, (**F**) three points for nonperipheral washout, (**G**) two points for blood products in mass, and (**H**) two points for AFP≥400ng/mL. The features were assessed, and a scoring model with continuous HRI-score was established to evaluate HRP in HCC. The threshold value of the HRI-score obtained via receiver operating characteristic curve analysis was used to predict HRP. When the HRI-score was greater than 4, it was considered positive; otherwise, it was considered negative.
Abbreviations: MRI, magnetic resonance imaging; AFP, α-fetoprotein; HCC, hepatocellular carcinoma; HRI, high-risk image feature.

Table 3 Verification of the HRI-Score for High-Risk and Low-Risk Pathologic Features

Parameter	Training Set	Internal Validation Set
AUC	0.813(0.778–0.849)	0.747(0.684–0.811)
Sensitivity	0.665(0.623–0.706)	0.713(0.650–0.775)
Specificity	0.870(0.804–0.936)	0.782(0.673–0.891)
PPV	0.962(0.942–0.982)	0.923(0.881–0.965)
NPV	0.341(0.283–0.399)	0.426(0.329–0.522)
Accuracy	0.699(0.660–0.735)	0.728(0.669–0.781)

Abbreviations: AUC, Area under the receiver operating characteristic curve; PPV, Positive predictive value; NPV, Negative predictive value.

RFS (HRP−/HRI− > HRP−/HRI+ > HRP+/HRI− > HRP+/HRI+). Importantly, patients who are HRI-positive demonstrated significantly worse outcomes than patients who are HRI-negative within the HRP-negative subgroup, suggesting that the HRI-score further improves risk stratification beyond pathological characteristics (Figure 3F and G).

Next, we assessed whether prognostic information beyond known clinicopathologic factors is carried by the HRI-score. HRI-positive status continued to be an independent predictor of worse RFS in multivariable Cox regression adjusted for known prognostic covariates (HR 1.51; 95% CI: 1.21–1.89, $P = 0.0003$) (Table 4).

Figure 3H and I present 3-D confusion matrices that illustrate how the HRI-score reclassifies patients in relation to pathologic HRP. A Sankey diagram of reclassification is displayed in Figure 4A. Interestingly, the scoring system reclassified 57 patients (7%) who were pathologically HRP-negative as HRI-positive, while 236 patients (28%) who were pathologically HRP-positive were reclassified as HRI-negative. These reclassifications imply that a subset of patients whose imaging/biomarker profile deviates from their pathology and who may experience different clinical outcomes are identified by the HRI-score. Particularly, the prevalence of HRI-positive status remained significant within frequently encountered early-stage populations: AFP < 400 ng/mL (46.4%, n = 652), AJCC T1 (53.8%, n = 459), CNLC T1 (55.9%, n = 499), and tumor size < 50 mm (48.9%, n = 519) (Figure 4B). These findings indicate that even among patients typically regarded as low-risk based on stage or AFP level, the HRI-score can detect "high-grade" biology.

Exploratory Analysis in the HRI-Negative Subgroup

Within the HRI-negative subgroup, patients with and without recurrence displayed significant differences in tumor shape ($P = 0.04$), nonrim arterial phase hyperenhancement ($P = 0.04$), nonperipheral washout ($P = 0.03$), and transient hepatic intensity ($P = 0.04$) (Table S7). These results indicate the possibility of residual heterogeneity among patients who are HRI-negative and suggest that additional imaging features could be useful for risk assessment.

Prediction of Adjuvant Therapy Benefit

We investigated whether patients who benefit from adjuvant therapies could be identified using the HRI-score. While RFS did not differ by adjuvant therapy when patients were grouped by pathologic HRP alone (HRP-positive or -negative; $P = 0.16$ and $P = 0.90$, respectively), HRI stratification revealed a differential effect: Among HRI-positive patients, receiving adjuvant therapy was associated with improved RFS (median RFS 74.0 versus 35.0 months; $P = 0.048$), while no benefit was observed in HRI-negative patients ($P = 0.43$) (Figure 5). This implies that patients who probably benefit from postoperative interventions may be chosen with the help of the imaging-biomarker signature.

We conducted subgroup analyses of various adjuvant strategies to investigate which adjuvant regimens might be effective within the HRI-positive population. When compared with other regimens, patients who receive TCM as part of their adjuvant regimen exhibit better RFS (Figure S2A and B). We used PSM to balance MVI status because baseline microvascular invasion varied between groups (Table S8); the correlation between TCM use and improved RFS persisted after PSM (Figure S2C), suggesting a potential therapeutic benefit. Since residual confounding cannot be completely ruled out, these findings are hypothesis-generating and should be interpreted cautiously.

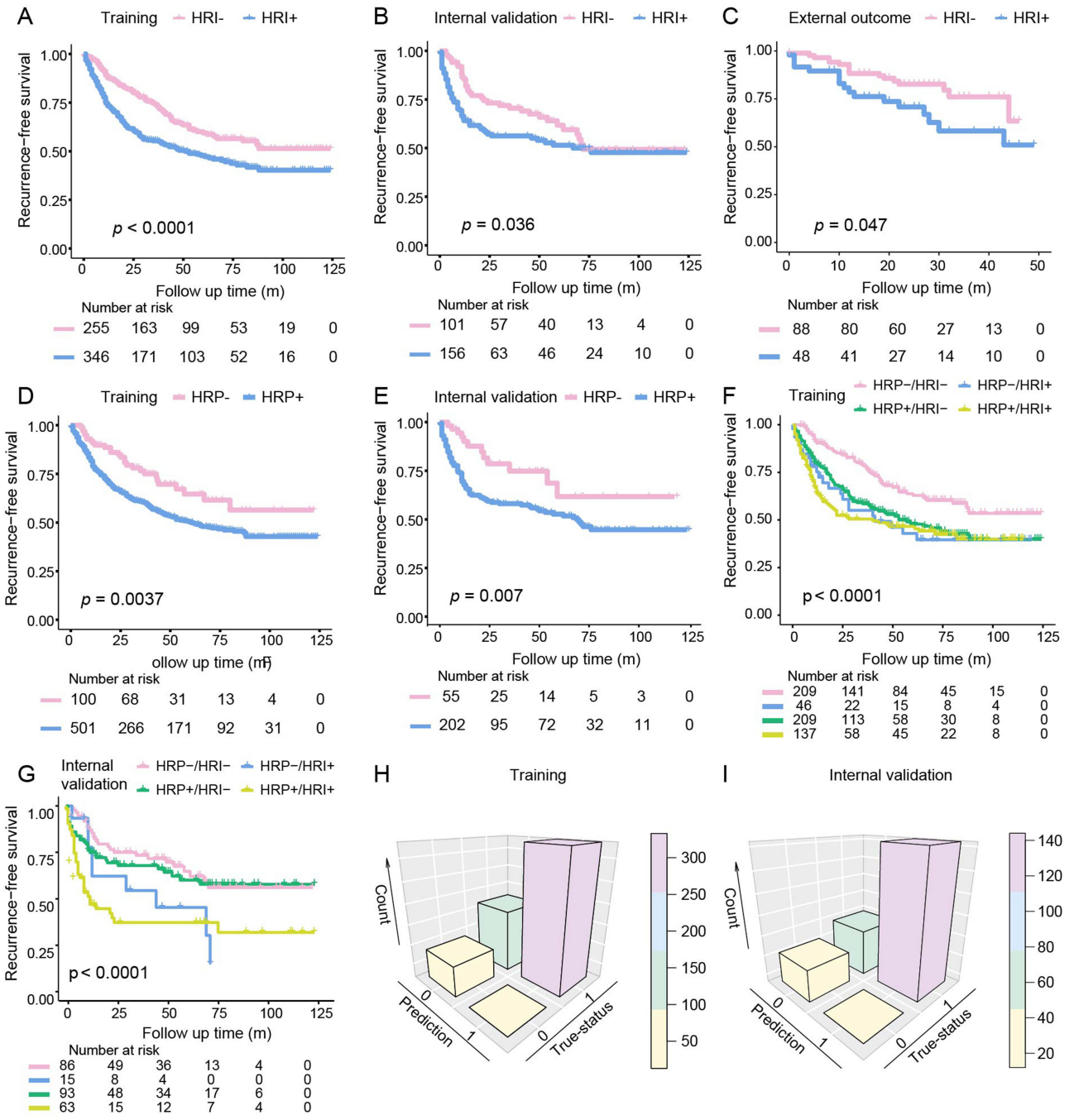

Figure 3 Kaplan–Meier analyses of recurrence-free survival (RFS) and model performance in patients with hepatocellular carcinoma. (**A–C**) RFS stratified by HRI-score (HRI− vs HRI+) in the training (A), internal validation (B), and external outcome (**C**) sets. (**D** and **E**) RFS stratified by high-risk pathological features (HRP− vs HRP+) in the training (**D**) and internal validation (**E**) sets. (**F** and **G**) Combined stratification of HRI-score and HRP status showing RFS differences among four subgroups (HRP−/HRI−, HRP−/HRI+, HRP+/HRI−, HRP+/HRI+) in the training (**F**) and internal validation (**G**) sets. (**H** and **I**) Confusion matrices of the HRI-score for predicting high-risk pathological features in the training (**H**) and internal validation (**I**) sets. HRI, high-risk image feature; HRP, high-risk pathologic feature. P values were calculated using the Log rank test. Numbers at risk are shown below each plot.

Discussion

This study highlights that preoperative noninvasive assessment of HRP in HCC is of significant clinical importance for prognostic evaluation and treatment decision-making. In this multicenter study involving 994 patients with BCLC stage 0/A HCC, we developed and validated a practical MRI-based scoring system (HRI-score) by combining preoperative AFP levels with standard LI-RADS imaging features. In both the training set (AUC = 0.813) and the internal validation

https://doi.org/10.2147/JHC.S605420

Table 4 Predictors for Recurrence Based on Cox Regression Analyses

Characteristics	Univariable		Multivariable	
	Hazard Ratio	P-value	Hazard Ratio	P-value
Sex (female vs. male)	1.37(1.03–1.81)	0.031	1.28(0.96–1.71)	0.0932
Age, years (< 65 vs. ≥65)	1.01(0.79–1.29)	0.938		
Aspartate aminotransferase, U/L (< 40 vs. ≥40)	**1.42(1.15–1.75)**	**0.001**	**1.25(1–1.55)**	**0.0465**
Alanine aminotransferase, U/L (< 50 vs. ≥50)	1.16(0.93–1.45)	0.178		
Gamma-glutamyl transferase, U/L (< 60 vs. ≥60)	1.47(1.2–1.81)	<0.001	1.23(0.98–1.53)	0.0706
Alkaline phosphatase, U/L (< 125 vs. ≥125)	1.04(0.77–1.4)	0.808		
Total bilirubin, umol/L (< 21 vs. ≥21)	1.12(0.86–1.46)	0.413		
Direct bilirubin, umol/L (< 3.4 vs. ≥3.4)	1.23(1–1.52)	0.054		
Cirrhosis (absent vs. present)	**1.4(1.03–1.9)**	**0.033**	**1.39(1.02–1.9)**	**0.0372**
Tumo number (unifocal vs. multifocal)	1.25(0.77–2.03)	0.371		
Tumor size, mm (< 50 vs. ≥50)	**1.67(1.35–2.05)**	**<0.001**	**1.45(1.17–1.8)**	**0.0008**
Adjuvant therapy (no vs. yes)	0.87(0.7–1.08)			
HRI (negative vs. positive)	**1.63(1.31–2.03)**	**<0.001**	**1.52(1.21–1.89)**	**0.0002**

Notes: Unless stated otherwise, data in parentheses are 95% confidence intervals. P values<0.05 are highlighted in bold. To avoid overfitting, variables with P<0.05 at the univariable Cox regression analyses were analyzed in the multivariable Cox regression models.
Abbreviation: HRI, high-risk image.

set (AUC = 0.747), the model demonstrated strong discriminative performance for HRP. More importantly, the HRI-score successfully identified patients at higher risk of postoperative recurrence and offered additional prognostic information beyond traditional clinicopathological factors.

Notably, with a comparatively high PPV, the HRI-score mainly serves as a "rule-in" tool, which makes it possible to identify patients with aggressive tumor biological behavior. However, it is inappropriate to consistently exclude low-risk individuals. We further examined postoperative recurrence in HRI-negative patients to overcome this limitation. The findings indicate that within this subgroup, imaging features such as tumor morphology, non-rim arterial phase hyperenhancement, nonperipheral washout, and transient hepatic parenchymal enhancement differ significantly between patients with and without recurrence. These results imply that patients who are HRI-negative still exhibit some degree of

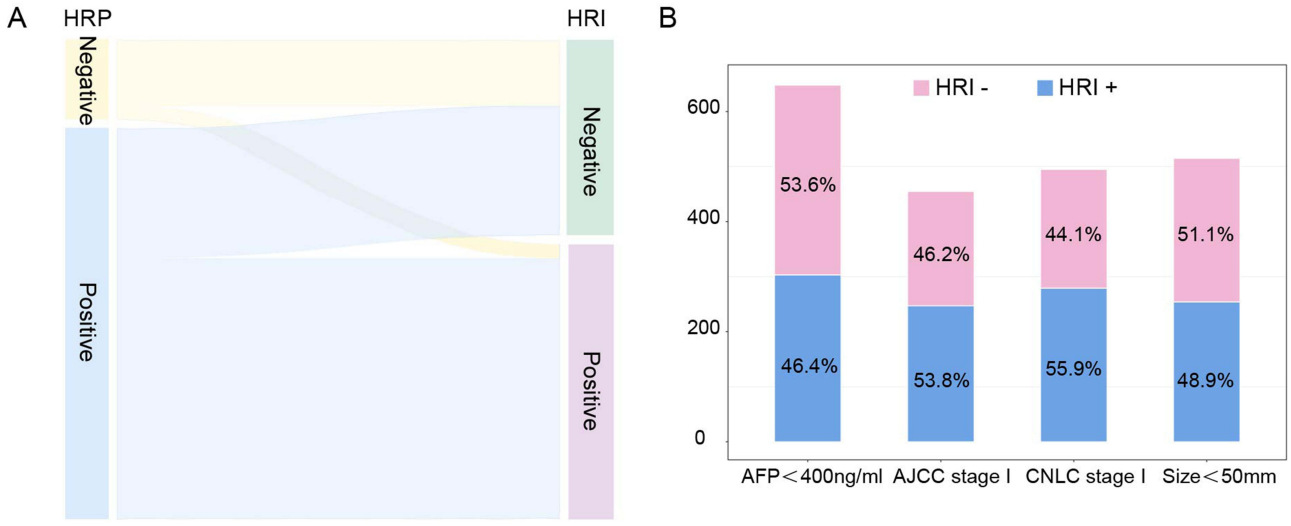

Figure 4 Distribution and stratification performance of the HRI-score in relation to HRP and clinical subgroups. (**A**) Sankey diagram illustrating the relationship between HRP status (negative vs positive) and HRI-score classification (HRI− vs HRI+). (**B**) Distribution of HRI-score (HRI− vs HRI+) across different clinical subgroups, including AFP level (<400 ng/mL), AJCC stage I, CNLC stage I, and tumor size (<50 mm). Proportions are presented within each subgroup.
Abbreviations: HRP, high-risk pathologic feature; HRI, high-risk image feature; AFP, α-fetoprotein; AJCC, American Joint Committee on Cancer; CNLC, China Liver Cancer Staging System.

https://doi.org/10.2147/JHC.S605420

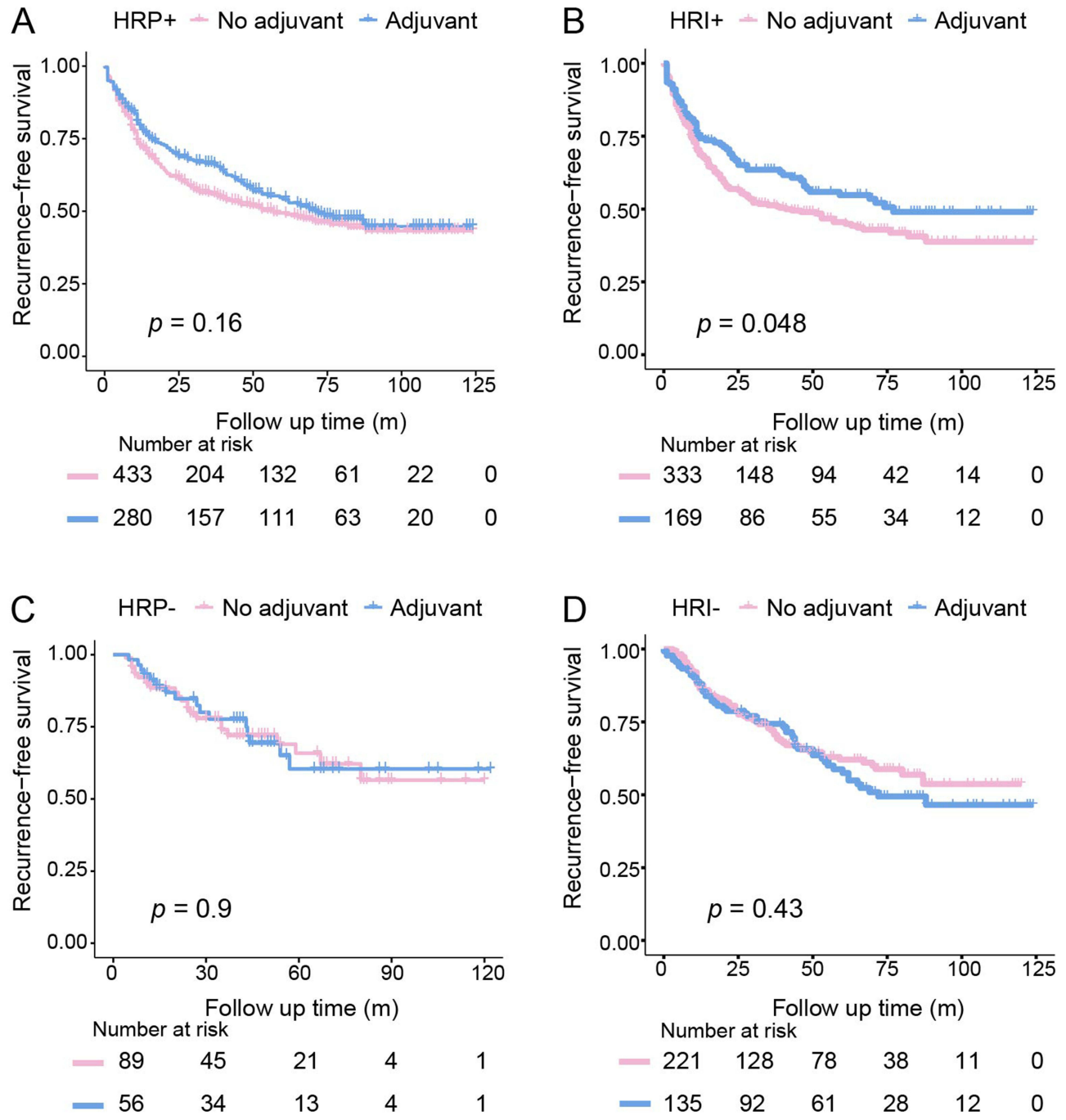

Figure 5 Association between adjuvant therapy and recurrence-free survival (RFS) stratified by HRP and HRI-score. (**A** and **B**) Kaplan–Meier curves of RFS comparing patients with and without adjuvant therapy in the HRP+ (**A**) and HRI+ (**B**) subgroups. (**C** and **D**) Kaplan–Meier curves of RFS comparing patients with and without adjuvant therapy in the HRP− (**C**) and HRI− (**D**) subgroups. P values were calculated using the Log rank test. Numbers at risk are shown below each plot.
Abbreviations: HRP, high-risk pathologic feature; HRI, high-risk image feature.

heterogeneity, and additional imaging features may offer complementary benefits for enhancing risk stratification. Consequently, to lower the risk of underestimation due to false-negative results, a thorough assessment that includes additional clinical and imaging data is still required for patients deemed low-risk by the HRI-score.

The HRI-score combines preoperative AFP levels with three LI-RADS imaging features: irregular tumor morphology, nonperipheral washout, and intratumoral hemorrhage. The feasibility and generalizability of the model are ensured by the fact that all of these variables are obtained from routine clinical examinations and exhibit strong reproducibility. Among

these, irregular tumor morphology was given a comparatively higher weight, which is in line with previous research demonstrating that this feature is closely associated with poor tumor differentiation, a higher Edmondson–Steiner grade, increased risk of MVI, and capsule disruption,[21] all of which are indicators of more aggressive tumor biological behavior. From a biological standpoint, irregular morphology could be a reflection of an infiltrative growth pattern and the tumor microenvironment's structural heterogeneity. The predominance of arterial blood supply within the tumor and decreased portal venous perfusion may be linked to nonperipheral washout, an important LI-RADS feature that causes rapid contrast washout during the portal venous phase.[22] This hemodynamic change is closely linked to tumor dedifferentiation and has been repeatedly demonstrated in this and previous studies to be correlated with lower RFS.[23] Additionally, it is generally believed that intratumoral hemorrhage is caused by rupture of newly formed vessels in rapidly growing tumors, which is an indirect reflection of increased angiogenic activity, hypoxic status, and invasive potential.[20,24] The most popular biomarker for HCC detection and surveillance is AFP. Tumor size, vascular invasion, and differentiation are all correlated with AFP levels.[25,26] The HRI-score offers a multidimensional assessment of tumor biological behavior by merging these imaging biomarkers with the traditional serum marker AFP. This imaging–biomarker integrated model provides a potent tool for preoperative risk stratification in early-stage HCC by enabling a more thorough and biologically significant assessment of tumor aggressiveness.

When compared to previous research, the current model demonstrates the clinical benefits of performing preoperative noninvasive assessment. Although several studies have suggested scoring systems based on postoperative pathological findings,[27] these methods cannot direct treatment choices before surgery. Contrastingly, the HRI-score fills the crucial gap by allowing risk stratification at a clinically actionable time point when treatment plans are still adjustable We discovered that while the HRI-score more accurately identified patients who actually benefited from adjuvant therapy, patients classified as "high-grade" according to postoperative pathological definitions did not always benefit from it. This implies that while preoperative models that include imaging and serological data may better capture a tumor's biological characteristics and support personalized treatment, traditional pathological assessment may fall short in accurately predicting treatment response. According to additional stratified analysis, RFS decreases in a stepwise manner across combined HRP and HRI groups (HRP−/HRI− > HRP−/HRI+ > HRP+/HRI− > HRP+/HRI+). This result suggests that traditional pathological features significantly supplement the HRI-score, allowing for additional improvements in patient stratification across various risk levels. Importantly, patients who are HRI-positive exhibited a significantly worse prognosis than patients who are HRI-negative, even within the HRP-negative subgroup, indicating that a subset of biologically aggressive tumors may go undetected by pathological evaluation alone, even in patients deemed low-risk. These findings indicate that the HRI-score enhances prognostic information provided by traditional pathological assessment instead of replacing it. This enhancement allows for more accurate and clinically significant risk stratification.

This study confirms earlier findings that adjuvant TCM therapy may enhance survival outcomes in specific high-risk patients after controlling for variations in BCLC stage 0/A. Notably, the HRI-score appears to work better as a "rule-in" tool for determining which patients would benefit from intensified treatment. The HRI-score has two significant uses from a clinical translation perspective. First, while patients who are HRI-negative may be treated with standard surgical approaches along with intensified postoperative surveillance, preoperative identification of patients who are HRI-positive may help surgeons consider more aggressive operative strategies, such as wider resection margins or anatomic hepatectomy. Second, our findings demonstrated that there was no significant survival benefit from adjuvant treatment when stratification was based only on pathological high-risk features. However, RFS significantly improves among patients who are HRI-positive following stratification using the HRI-score. This implies that imaging-based biomarkers could facilitate more accurate postoperative intervention strategies and help optimize patient selection. Significantly, adjuvant therapy regimens that included Huaier granules were linked to improved prognostic outcomes among patients who were HRI-positive. Huaier, a popular formulation in traditional Chinese medicine,[28,29] has been suggested to have antitumor effects through multiple mechanisms, such as regulating tumor proliferation, inducing apoptosis, and modulating the tumor immune microenvironment. Our results further support its potential benefit in this particular high-risk population after minimizing the impact of stage imbalance. However, these results should be interpreted cautiously. Residual confounding factors cannot be fully eliminated, given that the study was non-randomized. Therefore, these findings are mainly hypothesis-generating and need to be validated by future prospective multicenter studies.

This study has several limitations. First, using adjuvant therapy was decided by multidisciplinary individualized decision-making rather than being assigned randomly, which may introduce selection bias. Although PSM was used to adjust certain confounding factors, residual bias cannot be completely ruled out. Second, HBV infection was the main etiological factor, and the study population was entirely Chinese. Therefore, more research is required to validate the generalizability of the HRI-score and the therapeutic benefit of Huaier granules in other populations with various etiologies. To further confirm the results of this study, more extensive and prospective multicenter international research is required.

Conclusion

In conclusion, we developed a useful preoperative scoring system (HRI-score) that can noninvasively predict high-risk pathological features in BCLC 0/A HCC based on routine LI-RADS imaging features and preoperative AFP. This system enables preoperative prognostic stratification and precise identification of patients who may benefit from adjuvant therapy. The HRI-score offers new support for tailored treatment decisions in early-stage HCC as a simple, repeatable, and clinically accessible tool that may be enhanced with the potential to optimize clinical management and improve patient outcomes.

Statement of Ethics

The study received approval from the Ethics Committee of Harbin Medical University Cancer Hospital center (ID: KY2024-33). The committee waived the requirement for informed consent in view of the retrospective nature of the research and because it did not impactimpact on the clinical care of the patients involved. All procedures performed in the study were in strict adherence to the ethical standards outlined in the Declaration of Helsinki and its subsequent amendments.

Acknowledgments

Huiying Li and Xinxin Wang contributed equally as first authors; Yajuan Sun and Yang Zhou contributed equally as corresponding authors and last authors.

Author Contributions

All authors made a significant contribution to the work reported, whether that is in the conception, study design, execution, acquisition of data, analysis and interpretation, or in all these areas; took part in drafting, revising or critically reviewing the article; gave final approval of the version to be published; have agreed on the journal to which the article has been submitted; and agree to be accountable for all aspects of the work.

Funding

This work was supported by the Research Project of Health Commission of Heilongjiang Province (No. 20230909010304), and the Joint Fund Cultivation Project of Heilongjiang Provincial Natural Science Foundation (Grant No. PL2025H193).

Disclosure

The authors have no conflicts of interest to disclose.

References

1. Reig M, Forner A, Rimola J, et al. BCLC strategy for prognosis prediction and treatment recommendation: the 2022 update. *J Hepatol*. 2022;76(3):681–693. doi:10.1016/j.jhep.2021.11.018
2. Wang JH, Wang CC, Hung CH, Chen CL, Lu SN. Survival comparison between surgical resection and radiofrequency ablation for patients in BCLC very early/early stage hepatocellular carcinoma. *J Hepatol*. 2012;56(2):412–418. doi:10.1016/j.jhep.2011.05.020
3. Singal AG, Llovet JM, Yarchoan M, et al. AASLD practice guidance on prevention, diagnosis, and treatment of hepatocellular carcinoma. *Hepatology*. 2023;78(6):1922–1965. doi:10.1097/hep.0000000000000466
4. Chen ZX, Liu SY, Tong XM. Preoperative prediction of microvascular invasion: is invasive biopsy of HCC necessary? *J Hepatol*. 2022;77(3):892–893. doi:10.1016/j.jhep.2022.04.016
5. Martins-Filho SN, Paiva C, Azevedo RS, Alves VAF. Histological grading of hepatocellular carcinoma-a systematic review of literature. *Front Med*. 2017;4:193. doi:10.3389/fmed.2017.00193

6. Llovet JM, Pinyol R, Yarchoan M, et al. Adjuvant and neoadjuvant immunotherapies in hepatocellular carcinoma. *Nat Rev Clin Oncol*. 2024;21(4):294–311. doi:10.1038/s41571-024-00868-0
7. Sun J, Xia Y, Shen F, Cheng S. Chinese expert consensus on the diagnosis and treatment of hepatocellular carcinoma with microvascular invasion (2024 edition). *Hepatobiliary Surg Nutr*. 2025;14(2):246–266. doi:10.21037/hbsn-24-359
8. Zhou J, Sun H, Wang Z, et al. Guidelines for the diagnosis and treatment of primary liver cancer (2022 Edition). *Liver Cancer*. 2023;12(5):405–444. doi:10.1159/000530495
9. Chen Q, Shu C, Laurence AD, et al. Effect of Huaier granule on recurrence after curative resection of HCC: a multicentre, randomised clinical trial. *Gut*. 2018;67(11):2006–2016. doi:10.1136/gutjnl-2018-315983
10. Luo S, Hu H. Huaier granule prolongs overall survival after curative resection of hepatocarcinoma carcinoma: a propensity score analysis. *J Ethnopharmacol*. 2023;301:115774. doi:10.1016/j.jep.2022.115774
11. Wang Z, Yu XL, Zhang J, et al. Huaier granule prevents the recurrence of early-stage hepatocellular carcinoma after thermal ablation: a cohort study. *J Ethnopharmacol*. 2021;281:114539. doi:10.1016/j.jep.2021.114539
12. Li J, Xing J, Yang Y, et al. Adjuvant (131)I-metuximab for hepatocellular carcinoma after liver resection: a randomised, controlled, multicentre, open-label, Phase 2 trial. *Lancet Gastroenterol Hepatol*. 2020;5(6):548–560. doi:10.1016/s2468-1253(19)30422-4
13. Wang Z, Ren Z, Chen Y, et al. Adjuvant transarterial chemoembolization for HBV-related hepatocellular carcinoma after resection: a randomized controlled study. *Clin Cancer Res*. 2018;24(9):2074–2081. doi:10.1158/1078-0432.Ccr-17-2899
14. Li Y, Li P, Ma J, et al. Preoperative three-dimensional morphological tumor features predict microvascular invasion in hepatocellular carcinoma. *Acad Radiol*. 2024;31(5):1862–1869. doi:10.1016/j.acra.2023.10.060
15. Ronot M, Chernyak V, Burgoyne A, et al. Imaging to predict prognosis in hepatocellular carcinoma: current and future perspectives. *Radiology*. 2023;307(3):e221429. doi:10.1148/radiol.221429
16. Rong D, Liu W, Kuang S, et al. Preoperative prediction of pathologic grade of HCC on gadobenate dimeglumine-enhanced dynamic MRI. *Eur Radiol*. 2021;31(10):7584–7593. doi:10.1007/s00330-021-07891-0
17. Kim NR, Bae H, Hwang HS, et al. Preoperative prediction of microvascular invasion with gadoxetic acid-enhanced magnetic resonance imaging in patients with single hepatocellular carcinoma: the implication of surgical decision on the extent of liver resection. *Liver Cancer*. 2024;13(2):181–192. doi:10.1159/000531786
18. Sun Y, Yang H, Li S, et al. An accurate model for microvascular invasion prediction in solitary hepatocellular carcinoma ≤5 cm based on CEUS and EOB-MRI: a retrospective study with external validation. *Acad Radiol*. 2025;32(9):5173–5186. doi:10.1016/j.acra.2025.04.021
19. Vyas M, Zhang X. Hepatocellular carcinoma: role of pathology in the era of precision medicine. *Clin Liver Dis*. 2020;24(4):591–610. doi:10.1016/j.cld.2020.07.010
20. Cerny M, Chernyak V, Olivié D, et al. LI-RADS version 2018 ancillary features at MRI. *Radiographics*. 2018;38(7):1973–2001. doi:10.1148/rg.2018180052
21. Ariizumi S, Kitagawa K, Kotera Y, et al. A non-smooth tumor margin in the hepatobiliary phase of gadoxetic acid disodium (Gd-EOB-DTPA)-enhanced magnetic resonance imaging predicts microscopic portal vein invasion, intrahepatic metastasis, and early recurrence after hepatectomy in patients with hepatocellular carcinoma. *J Hepatobiliary Pancreat Sci*. 2011;18(4):575–585. doi:10.1007/s00534-010-0369-y
22. Choi JY, Lee JM, Sirlin CB. CT and MR imaging diagnosis and staging of hepatocellular carcinoma: part I. Development, growth, and spread: key pathologic and imaging aspects. *Radiology*. 2014;272(3):635–654. doi:10.1148/radiol.14132361
23. Jiang H, Qin Y, Wei H, et al. Prognostic MRI features to predict postresection survivals for very early to intermediate stage hepatocellular carcinoma. *Eur Radiol*. 2024;34(5):3163–3182. doi:10.1007/s00330-023-10279-x
24. Wang L, Feng B, Liang M, et al. Prognostic performance of MRI LI-RADS version 2018 features and clinical-pathological factors in alpha-fetoprotein-negative hepatocellular carcinoma. *Abdom Radiol*. 2024;49(6):1918–1928. doi:10.1007/s00261-024-04278-9
25. Galle PR, Foerster F, Kudo M, et al. Biology and significance of alpha-fetoprotein in hepatocellular carcinoma. *Liver Int*. 2019;39(12):2214–2229. doi:10.1111/liv.14223
26. Ma C, Jin Y, Wang Y, Xu H, Zhang J. Beyond liver cancer, more application scenarios for alpha-fetoprotein in clinical practice. *Front Oncol*. 2023;13:1231420. doi:10.3389/fonc.2023.1231420
27. Xia F, Yan J, Liu X, et al. A novel pathologic scoring system for predicting postoperative recurrence in BCLC stage 0-A hepatocellular carcinoma patients: a nationwide multicenter study. *Sci China Life Sci*. 2025;69(2):611–621. doi:10.1007/s11427-025-3045-1
28. Song X, Li Y, Zhang H, Yang Q. The anticancer effect of Huaier (Review). *Oncol Rep*. 2015;34(1):12–21. doi:10.3892/or.2015.3950
29. Wang X, Zhang N, Huo Q, Yang Q. Anti-angiogenic and antitumor activities of Huaier aqueous extract. *Oncol Rep*. 2012;28(4):1167–1175. doi:10.3892/or.2012.1961